Stochastic model of nanomechanical electron shuttles and symmetry breaking

Mo Zhao[1] and Robert H. Blick[1,2,3,*]

[1]*Department of Electrical & Computer Engineering, University of Wisconsin–Madison, Madison, Wisconsin 53706, USA*

[2]*Center for Hybrid Nanostructures, Falkenried 88, 20251 Hamburg, Germany*

[3]*Institutes for Nanostructure and Solid State Physics, University of Hamburg, 20355 Hamburg, Germany*

(Received 25 July 2015; revised manuscript received 16 May 2016; published 14 June 2016)

Nanomechanical electron shuttles can work as ratchets for radio-frequency rectification. We develop a full stochastic model of coupled shuttles, where the mechanical motion of nanopillars and the incoherent electronic tunneling are modeled by a Markov chain. In particular, the interaction of their randomness is taken into account, so that a linear master equation is constructed. Numerical solutions from our fast approximate method and analytical derivation reveal the symmetry breaking, which results in the direct current observed in earlier measurements [Phys. Rev. Lett. **105**, 067204 (2010)]. Additionally, the method can facilitate device simulation of more complex designs such as shuttle arrays.

DOI: 10.1103/PhysRevE.93.063306

I. INTRODUCTION

Nanoelectromechanical systems have attracted significant interest in the past decade because they can provide a number of promising applications [1]. Among them, the nanomechanical electron shuttle proposed by Gorelik *et al.* is an outstanding example that received considerable theoretical [2–22] and experimental [23–34] attention. The shuttle is typically realized by metallic islands, quantum dots, or large molecules and can be excited by a radio-frequency (RF) voltage so that electrons are shuttled between electrodes. Due to strong nonlinear electro-mechanical coupling, such devices can be used as RF modulators or as a high-frequency current ratchet. It was shown that single and, more effectively, coupled electron shuttles can rectify applied RF signals and give rise to a direct current that may be used to power electronic devices [21,22,31–33]. While previous theoretical studies provide fundamental insights into the physics, we are still unable to make accurate predictions on the device level.

In this paper, we focus on modeling coupled electron shuttles that would greatly favor energy scavenging. As shown in Fig. 1(a), the coupled electron shuttles oscillate between the source and drain electrodes with alternating voltage $V(t)$ (additional gate electrodes with constant charges can be applied), triggering nonresonant electron tunneling. The size of shuttles is generally 1–100 nm, and they work at room temperature. Figure 1(b) shows a typical design where the oscillation of shuttles is restrained by the supporting nanopillars' eigenmodes. Thus, we develop a new model based on the semiclassical stochastic theory that enables analytical and numerical analysis of the device. This is important for designing practical energy scavengers, where arrays of electron shuttles are coupled to generate an appreciable output current.

Because the incoherent tunneling is dominant in such scenarios [35], the electron tunneling and the shuttle oscillation in the system can be modeled as a continuous stochastic process. Thus, a semiclassical statistical model is more suitable than the full quantum-mechanical treatments [15–19], which work better for coherent devices. In the following, we develop a linear master equation describing the probability distribution of the electron numbers in the shuttles. Although the probability distribution was widely discussed in previous studies on the single shuttle [2,3,8–14], most approaches describe the mechanical oscillation by deterministic variables and their master equation is nonlinear.

Ahn [21] and Prada [22] extended such approaches to pioneer the modeling of the coupled shuttles. In contrast to some earlier models [6–11,14], they allow electron numbers in a shuttle to be greater than one. Our model follows their assumptions, but the linear master equation enables further analytical study. More importantly, we propose the approximate deterministic equations for the mean and deviation of physical quantities, from which we can compute the macroscopic direct current. This brings the large-scale device simulation to a level of acceptable speed and accuracy.

II. FULL STOCHASTIC MODEL

We describe the displacement and velocity of the sth shuttle ($s = 1,2$) at the time t by random variables $\tilde{x}_s(t)$ and $\tilde{v}_s(t)$, and describe the number of net electrons in the shuttle by the integer-valued random variable $\tilde{n}_s(t)$. For simplicity, we write them by vectors $\tilde{\boldsymbol{x}}(t), \tilde{\boldsymbol{v}}(t)$, and $\tilde{\boldsymbol{n}}(t)$ [typically "(t)" is omitted in the following]. We assume these three random variables are sufficient to describe the immediate state of the system and evolute as a Markov chain. The mean of a random variable is noted by a bracket, e.g., $\langle\tilde{\boldsymbol{x}}(t)\rangle$ or simply $\langle\tilde{\boldsymbol{x}}\rangle$. Also we assume a constant number of electrons on the gate electrodes noted by vector $\boldsymbol{n}_{\mathrm{G}}$. We use $P(\boldsymbol{n},\boldsymbol{x},\boldsymbol{v},t)$ to describe the joint probability distribution function (PDF) of $\tilde{\boldsymbol{n}}(t)$, $\tilde{\boldsymbol{x}}(t)$, and $\tilde{\boldsymbol{v}}(t)$, whose variables $\boldsymbol{n},\boldsymbol{x}$, and $\boldsymbol{v}$ have the same value range as these random variables.

Assuming the sth pillar has an eigenfrequency ω_s, effective mass m_s, and damping coefficient $\gamma_s = \omega_s/Q$ with Q being the quality factor, we have $\tilde{x}_s(t)$ and $\tilde{v}_s(t)$ satisfying the following stochastic differential equations:

$$\begin{aligned} d\tilde{x}_s/dt &= \tilde{v}_s, \\ d\tilde{v}_s/dt &= -\gamma_s\tilde{v}_s - \omega_s^2\tilde{x}_s + F_s(\tilde{\boldsymbol{n}},t)/m_s, \end{aligned} \tag{1}$$

*robert@nanomachines.com

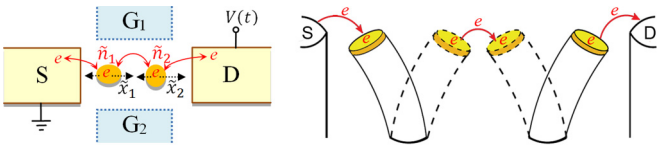

(a) (b)

FIG. 1. (a) Coupled nanomechanical electron shuttles, set with electrodes S, D and optionally G1, G2, oscillate under driving voltage and have electrons tunneled. (b) Side view of a typical design where shuttles are on top of nanopillars.

where F_s is the electromagnetic force on the sth shuttle and can be approximated as a function of $\tilde{\boldsymbol{n}}(t)$ and $V(t)$. Since the probability distribution of $\tilde{\boldsymbol{n}}(t)$ is unknown, we cannot simply solve the equations to describe $\tilde{x}_s(t)$ and $\tilde{v}_s(t)$. Instead, assuming $P(\boldsymbol{n},\boldsymbol{x},\boldsymbol{v},t)$ changes to $P(\boldsymbol{n}',\boldsymbol{x}',\boldsymbol{v}',t')$ after infinitesimal time $\Delta t = t' - t$, from Eq. (1) which implies deterministic change of motion, we can write the conditional probability in the form of Dirac delta functions:

$$P(x_s',v_s',t'|\boldsymbol{n},\boldsymbol{x},\boldsymbol{v},t) = \delta(x_s' - x_s - v_s\Delta t) \cdot \delta\big(v_s' - v_s + \big[\gamma_s\tilde{v}_s + \omega_s^2\tilde{x}_s - F_s(\tilde{\boldsymbol{n}},t)/m_s\big]\Delta t\big) + o(\Delta t), \tag{2}$$

where $o(\Delta t)$ denotes a high-order infinitesimal of Δt.

Another mechanism restraining the PDF besides the mechanical motion is the tunneling of electrons, which can be modeled by the orthodox model [6]. The components of $\boldsymbol{n} - \boldsymbol{n}'$ are limited to ± 1 and 0 for considering single electron tunneling at each step. Technically we define a vector $\boldsymbol{\mu}$, whose components μ_j denote the number of electron tunneled through the jth junction ($j = 1,2,3$) and can be 0 and ± 1. We also define

$$\boldsymbol{T} = \begin{bmatrix} 1 & 0 \\ -1 & 1 \\ 0 & -1 \end{bmatrix}, \tag{3}$$

so that $\boldsymbol{n} = \boldsymbol{n}' - \boldsymbol{\mu}\boldsymbol{T}$ and note its jth row by a vector $\boldsymbol{T}_j$. The transition probability of μ_j electrons tunneling through the jth junction is

$$P(\mu_j,t'|\boldsymbol{n},\boldsymbol{x},t) = \begin{cases} \Gamma_j^{\pm}\Delta t, & \mu_j = \pm 1, \\ 1 - (\Gamma_j^{+} + \Gamma_j^{-})\Delta t, & \mu_j = 0, \end{cases} \tag{4}$$

where

$$\Gamma_j^{\pm}(\boldsymbol{n},\boldsymbol{x},t) = \frac{e^{-\boldsymbol{x}\cdot\boldsymbol{T}_j/\lambda_j}}{q^2R_j^0}\frac{U_j^{\pm}}{1 - e^{-U_j^{\pm}/k_BT}} \tag{5}$$

is the forward or backward (+ or −) tunneling rate of electrons through the jth junction, wherein R_j^0 is the unperturbed tunneling resistance from the mechanical motions, λ_j is the tunneling wavelength, T is the temperature, k_B is the Boltzmann constant, and $U_j^{\pm}$ denotes the change of electromagnetic energy due to the tunneling.

The electromagnetic field can be modeled by the partial capacitance matrix due to the geometry that makes the inductance (or variation of the magnetic energy) negligible. Thus, the energy E_C stored in the field should be a homogeneous second-order polynomial of the charges $q\boldsymbol{n}(t), q\boldsymbol{n}_G$ and the applied voltage $V(t)$, with coefficients associated with the partial capacitance. Comparing the formula of E_C before and after the tunneling, we obtain the unperturbed $U_j^{\pm}$:

$$U_j^{\pm}(\boldsymbol{n},t) = -E_j^0 \mp (\boldsymbol{E}^0\boldsymbol{\Theta}_j)\cdot(\boldsymbol{n} - \boldsymbol{n}_G\boldsymbol{B}) \pm q\kappa_j V(t), \tag{6}$$

where E_j^0 is the jth component of $\boldsymbol{E}^0$ ($j = 1,2,3$) denoting the ground-state energies, $\boldsymbol{B}$ is a unitless matrix to describe the effect of gate bias, and κ_j is a unitless coefficient representing the number of electrons pumped between the electrodes by an outside voltage source when an electron tunnels through the jth junction, satisfying $\kappa_1 + \kappa_2 + \kappa_3 = 1$. Their values are determined by the capacitance matrix associated with geometry and material [36]. In addition, $\boldsymbol{\Theta}_j$ is a constant matrix:

$$\boldsymbol{\Theta}_1 = \begin{bmatrix} 2 & 1 \\ 0 & -1 \\ 0 & 1 \end{bmatrix}, \quad \boldsymbol{\Theta}_2 = \begin{bmatrix} -1 & -1 \\ -1 & 1 \\ 1 & 1 \end{bmatrix}, \quad \boldsymbol{\Theta}_3 = \begin{bmatrix} -1 & 0 \\ 1 & 0 \\ -1 & -2 \end{bmatrix}.$$

The electric force on the sth shuttle ($s = 1,2$) is $F_s = -\partial E_C/\partial x_s$. Take the first-order Taylor expansion of E_C and ignore the dependence of F_s on x_s. We get

$$F_s(\tilde{\boldsymbol{n}},t) = \tilde{\boldsymbol{n}}\boldsymbol{F}_s^0\tilde{\boldsymbol{n}}^T + \tilde{\boldsymbol{n}}\boldsymbol{F}_s^G\boldsymbol{n}_G^T + \boldsymbol{n}_G\boldsymbol{F}_s^{GG}\boldsymbol{n}_G^T + q\big(\tilde{\boldsymbol{n}}\cdot\boldsymbol{\alpha}_s + \boldsymbol{n}_G\cdot\boldsymbol{\alpha}_s^G\big)V(t), \tag{7}$$

where $\boldsymbol{F}_s^0, \boldsymbol{F}_s^G$, and $\boldsymbol{F}_s^{GG}$ are matrices of constant force related to geometry and material (the matrix dimensions are consistent with their multipliers $\tilde{\boldsymbol{n}}$ or $\boldsymbol{n}_G$ to make F_s a scalar), and $\boldsymbol{\alpha}_s$ and $\boldsymbol{\alpha}_s^G$ are constant vectors representing the reciprocal length. These parameters result from spatial derivatives of the capacitance matrix. Note that α_{ss}, the sth component of the vector $\boldsymbol{\alpha}_s$, is usually much larger than other components. If $\boldsymbol{n}_G = 0$, we could drop the small terms and use $F_s \cong q\tilde{n}_s\alpha_{ss}V(t)$, which is linear to $\tilde{n}_s$ and consistent with the assumption in Ref. [21]. For large $\boldsymbol{n}_G, F_s \cong q\boldsymbol{n}_G\cdot\boldsymbol{\alpha}_s^G V(t)$ is a fair approximation.

The white noise can be added to Eq. (7) to account for heating effects, but its energy $k_BT/2$ is usually far too small compared to the electric driving vibrations.

For the first-order perturbation for $\boldsymbol{x}, E_C$ should be subtracted by $\boldsymbol{F}(\boldsymbol{n},t)\cdot\boldsymbol{x}$, where $\boldsymbol{F} = [F_1,F_2]$ is the force vector on shuttles. For $\boldsymbol{n}_G = 0$, we have

$$U_j^{\pm}(\boldsymbol{n},\boldsymbol{x},t) \cong U_j^{\pm}(\boldsymbol{n},t) \mp \big[qV(t)\bar{\boldsymbol{\alpha}}_j + \boldsymbol{n}\bar{\boldsymbol{F}}_j^0\big]\cdot\boldsymbol{x},$$

where $\bar{\boldsymbol{F}}_j^0 = [\boldsymbol{F}_1^0\boldsymbol{T}_j^T, \boldsymbol{F}_2^0\boldsymbol{T}_j^T]$, $\bar{\boldsymbol{\alpha}}_j = \boldsymbol{T}_j[\boldsymbol{\alpha}_1^T, \boldsymbol{\alpha}_2^T]$. For $\boldsymbol{n}_G \neq 0$, we further add $\mp\boldsymbol{T}_j[\boldsymbol{F}_1^G\boldsymbol{n}_G^T, \boldsymbol{F}_2^G\boldsymbol{n}_G^T]\cdot\boldsymbol{x}$ to U_j.

Because the electron tunneling through each junction and the mechanical motion of each shuttle are independent, we have the Chapman-Kolmogorov equation [36]:

$$P(\boldsymbol{n}',\boldsymbol{x}',\boldsymbol{v}',t') = \sum_{\mu_j=0,\pm 1}\int P(\boldsymbol{n},\boldsymbol{x},\boldsymbol{v},t)\prod_{j=1}^{3}P(\mu_j,t'|\boldsymbol{n},\boldsymbol{x},t) \cdot\prod_{s=1}^{2}P(x_s',v_s',t'|\boldsymbol{n},\boldsymbol{x},\boldsymbol{v},t)\,d\Omega, \tag{8}$$

where $d\Omega = dx_1\,dx_2\,dv_1\,dv_2$. From Eq. (2), (4), and (8), we can describe the time derivative of the PDF by adopting the limit $t' \to t$. Note that a strict derivation should consider a mixed moment of displacement and velocity instead of using Eq. (2), which is covered by Ref. [36]. We hence build the following master equation for $P(\boldsymbol{n},\boldsymbol{x},\boldsymbol{v},t)$:

$$\frac{\partial P}{\partial t} = \sum_{j=1}^{3}\sum_{\pm}(\hat{\mathcal{N}}_{\mp \boldsymbol{T}_j} - 1)\Gamma_j^{\pm} P + \sum_{s=1}^{2}\left\{\gamma_s P - v_s\frac{\partial P}{\partial x_s} + \left[\gamma_s v_s + \omega_s^2 x_s - \frac{F_s(\boldsymbol{n},t)}{m_s}\right]\frac{\partial P}{\partial v_s}\right\}, \tag{9}$$

where the operator $\hat{\mathcal{N}}_{\mp \boldsymbol{T}_j}$ shifts the argument $\boldsymbol{n}$ in a function by $\mp \boldsymbol{T}_j$. Equation (9) is a linear first-order partial differential equation. Its boundary condition is implicit, i.e., as $|n_s| \to \infty$ or $|x_s| \to \infty$ or $|v_s| \to \infty, P(\boldsymbol{n},\boldsymbol{x},\boldsymbol{v},t) \to 0$ (asymptotically as a Gaussian function). In addition, Eq. (9) is homogeneous, so the solution is linear with the initial condition, in which the PDF should be normalized. Given an initial condition, we can solve the equation to obtain a conditional PDF. Nevertheless, we are more interested in the steady-state solution in which the PDF becomes periodic and irrelevant to the initial PDF after numerous periods (so that the initial condition only plays a role in normalization). From numerical solutions, we learn that such a PDF (at a specific time) is usually very close to a multivariate Gaussian distribution [36]. This conclusion complies with the central limit theorem under weak dependence, because the stochastic process consists of infinite times of single electron tunneling which are weakly dependent on others.

Although Eq. (9) with linear properties is meaningful for analysis, it is very difficult to solve numerically with good accuracy (like the Monte Carlo method and the method of lines), because the PDF has as many as seven arguments. Ignoring the generally weak correlation of $\tilde{\boldsymbol{n}}(t)$ and $\tilde{\boldsymbol{x}}(t)$ and the relatively small variance of $\tilde{\boldsymbol{x}}(t)$, we can integrate Eq. (9) over x_1,x_2,v_1,v_2 to transform into a simpler equation for the marginal distribution $P(\boldsymbol{n},t) = \int P(\boldsymbol{n},\boldsymbol{x},\boldsymbol{v},t)\,d\Omega$:

$$\frac{\partial P(\boldsymbol{n},t)}{\partial t} = \sum_{j=1}^{3}\sum_{\pm}\left(\hat{\mathcal{N}}_{\mp \boldsymbol{T}_j} - 1\right)\Gamma_j^{\pm}(\boldsymbol{n},\langle\tilde{\boldsymbol{x}}\rangle,t)P(\boldsymbol{n},t), \tag{10}$$

where $\langle\tilde{\boldsymbol{x}}\rangle$ can be linked to $\langle F_s(\tilde{\boldsymbol{n}},t)\rangle$ by the mean of Eq. (1). In fact, this is equivalent to the master equation given in Refs. [21] and [22]. The disadvantage is that the equation is nonlinear as the relation of $\langle\tilde{\boldsymbol{x}}\rangle$ and $P(\boldsymbol{n},t)$ is implicit. Without linearity, we can hardly discuss the analytical solution, since superposition of initial conditions and solutions are disallowed. For numerical solutions, challenge is normalization of the PDF and convergence and accuracy after a long time. In addition, the approximation does not cover the resonance scenario where $\max\langle\tilde{\boldsymbol{x}}(t)\rangle \gg \lambda_j$.

III. DEVICE-LEVEL SIMULATION

A. Approximate solution for means and variances

We are more interested in the measurable physical quantities which are the mean values of the random variables rather than the PDF. Without solving the PDF, we can build deterministic equations for the mean from Eq. (9) as well and solve them as time-dependent functions. By multiplying n_s to both sides of Eq. (9), $s = 1,2$, and summing over $\boldsymbol{n},\boldsymbol{x},\boldsymbol{v}$, we obtain

$$\frac{d\langle\tilde{n}_s\rangle}{dt} = \sum_{j=1}^{3} T_{js}\langle\Gamma_j(\tilde{\boldsymbol{n}},\tilde{\boldsymbol{x}},t)\rangle, \tag{11}$$

where $\Gamma_j = \Gamma_j^{+} - \Gamma_j^{-}$, and T_{js} is a matrix element of $\boldsymbol{T}$.

Let us first consider a simple approximation: use the unperturbed $\langle U_j^{\pm}(\tilde{\boldsymbol{n}},t)\rangle$ and assume its mean has an absolute value much larger than $k_{\mathrm{B}}T$; ignore the correlation of $\tilde{\boldsymbol{n}}(t)$ and $\tilde{\boldsymbol{x}}(t)$ and the variance of $\tilde{\boldsymbol{x}}(t)$. Then $\Gamma_j(\tilde{\boldsymbol{n}},t) \approx U_j(\tilde{\boldsymbol{n}},t)/(q^2R_j^0)$, where

$$\begin{aligned} U_j(\tilde{\boldsymbol{n}},t) &= [U_j^{+}(\tilde{\boldsymbol{n}},t) - U_j^{-}(\tilde{\boldsymbol{n}},t)]/2 \\ &= q\kappa_j V(t) - (\tilde{\boldsymbol{n}} - \boldsymbol{n}_{\mathrm{G}}\boldsymbol{B})\cdot(\boldsymbol{E}^0\boldsymbol{\Theta}_j) \end{aligned}$$

is a linear function of $\tilde{\boldsymbol{n}}$. We can replace Eq. (11) by

$$\frac{d\langle\tilde{n}_s\rangle}{dt} \cong \sum_{j=1}^{3}\frac{T_{js}}{q^2R_j^0}\mathrm{e}^{-\langle\tilde{\boldsymbol{x}}\rangle\cdot\boldsymbol{T}_j/\lambda_j}U_j(\langle\tilde{\boldsymbol{n}}\rangle,t). \tag{12}$$

This can be combined with the mean of Eq. (1) to solve $\langle\tilde{\boldsymbol{x}}\rangle$ and $\langle\Gamma_j\rangle$. In fact, Eq. (12) can be interpreted as a circuit model composed by capacitors and resistors, and the model can even more be simplified by ignoring the charging current of capacitors (i.e., $\partial\langle\tilde{n}_s\rangle/\partial t = 0$) to comply with the adiabatic-limit model in Ref. [21]. However, this simple circuit model does not hold with a high-frequency excitation and is too rough for simulation of the current.

For higher accuracy, we may assume $\tilde{n}_s,\tilde{x}_s$, and $\tilde{v}_s$ $(s = 1,2)$ have the multivariate Gaussian distribution. If the covariance matrices of $\tilde{\boldsymbol{n}},\tilde{\boldsymbol{x}}$, and $\tilde{\boldsymbol{v}}$ are denoted by $\boldsymbol{D},\boldsymbol{\Lambda}$, and $\boldsymbol{V}$, respectively, we can use the Taylor expansion of $\Gamma_j^{\pm}(\tilde{\boldsymbol{n}},\tilde{\boldsymbol{x}},t)$ for $\tilde{\boldsymbol{n}}$ and $\tilde{\boldsymbol{x}}$ near their means to obtain

$$\begin{aligned} \langle\Gamma_j^{\pm}(\tilde{\boldsymbol{n}},\tilde{\boldsymbol{x}},t)\rangle \cong\ & \frac{1}{q^2R_j^0}\mathrm{e}^{-\langle\tilde{\boldsymbol{x}}\rangle\cdot\boldsymbol{T}_j/\lambda_j}\mathrm{e}^{\boldsymbol{T}_j\boldsymbol{\Lambda}\boldsymbol{T}_j^{\mathrm{T}}/\lambda_j^2} \\ & \cdot\sum_{l_1,l_2=0}^{\infty}\frac{(\mp 1)^{l_1+l_2}}{l_1!\,l_2!}E_{1j}^{l_1}E_{2j}^{l_2}\cdot Y_{l_1+l_2}(U_j^{\pm}(\langle\boldsymbol{n}\rangle,\langle\boldsymbol{x}\rangle,t))M_{l_1l_2}, \end{aligned} \tag{13}$$

where $Y_l(U) = \partial^l[U/(1-\mathrm{e}^{-U/k_{\mathrm{B}}T})]/\partial U^l$, E_{1j} and E_{2j} are components of $\boldsymbol{E}^0\boldsymbol{\Theta}_j$, and $M_{l_1l_2}$ is the l_1,l_2-order mixed moment of n_1,n_2 following the Isserlis theorem:

$$M_{l_1l_2} = \langle(\tilde{n}_1 - \langle\tilde{n}_1\rangle)^{l_1}(\tilde{n}_2 - \langle\tilde{n}_2\rangle)^{l_2}\rangle = \begin{cases} \sum_{k=0}^{l_{\mathrm{m}}}\frac{l_1!\,l_2!D_{11}^{\frac{l_1}{2}-k}D_{22}^{\frac{l_2}{2}-k}}{(l_1-2k)!!(l_2-2k)!!}\frac{D_{12}^{2k}}{(2k)!}, & l_1,l_2 \text{ even} \\ \sum_{k=0}^{l_{\mathrm{m}}}\frac{l_1!\,l_2!D_{11}^{\frac{l_1-1}{2}-k}D_{22}^{\frac{l_2-1}{2}-k}}{(l_1-1-2k)!!(l_2-1-2k)!!}\frac{D_{12}^{2k+1}}{(2k+1)!}, & l_1,l_2 \text{ odd} \\ 0, & l_1+l_2 \text{ odd} \end{cases}, \tag{14}$$

where $l_{\rm m}$ denotes the integer part of $\min(l_1,l_2)/2$. We can also build equations for the variance and the covariance:

$$\frac{dD_{ss}}{dt} = \sum_{j=1}^{3}\left[2T_{js}\langle\Gamma_j(\tilde{\boldsymbol{n}},\tilde{\boldsymbol{x}},t)(\tilde{n}_s-\langle\tilde{n}_s\rangle)\rangle + T_{js}^2\langle\Gamma_j^*(\tilde{\boldsymbol{n}},\tilde{\boldsymbol{x}},t)\rangle\right], \tag{15}$$

$$\frac{dD_{12}}{dt} = \sum_{j=1}^{3}\sum_{s=1}^{2} T_{j(3-s)}\langle\Gamma_j(\tilde{\boldsymbol{n}},\tilde{\boldsymbol{x}},t)(\tilde{n}_s-\langle\tilde{n}_s\rangle)\rangle - \langle\Gamma_2^*(\tilde{\boldsymbol{n}},\tilde{\boldsymbol{x}},t)\rangle, \tag{16}$$

where $\Gamma_j^* = \Gamma_j^+ + \Gamma_j^-$. The result of $\langle\Gamma_j(\tilde{\boldsymbol{n}},t)(\tilde{n}_s-\langle\tilde{n}_s\rangle)\rangle$ is similar to the right side of Eq. (13) with $M_{l_1l_2}$ replaced by M_{l_1+1,l_2} or M_{l_1,l_2+1} according to $s = 1,2$.

Further, assume Σ_s as the covariance of $\tilde{x}_s$ and $\tilde{v}_s$, X_s as the covariance of $\tilde{x}_s$ and $\tilde{n}_s$, and Y_s as the covariance of $\tilde{n}_s$ and $\tilde{v}_s$. Other covariances which are between different shuttles are generally negligible, due to small correlation between $F_s(\tilde{\boldsymbol{n}},t)$ and $\tilde{n}_{s'}$ ($s \neq s'$), i.e., $\alpha_{ss} \gg \alpha_{ss'}$. Multiply Eq. (9) with x_s and x_s^2 and sum over $\boldsymbol{n},\boldsymbol{x},\boldsymbol{v}$, so we can derive $d\langle\tilde{x}_s\rangle/dt = \langle\tilde{v}_s\rangle$ and $d\langle\tilde{x}_s^2\rangle/dt = 2\langle\tilde{x}_s\tilde{v}_s\rangle$, respectively. By combining them, we obtain

$$\frac{d\Lambda_{ss}}{dt} = 2\Sigma_s. \tag{17}$$

Similarly, we can build equations describing the time derivative of W_s,Σ_s,X_s, and Y_s [36]:

$$\frac{dW_s}{dt} = 2\left[-\gamma_s W_s - \omega_s^2\Sigma_s + Y_s\frac{\langle f_s(\tilde{\boldsymbol{n}},t)\rangle}{m_s}\right], \tag{18}$$

$$\frac{d\Sigma_s}{dt} = W_s - \gamma_s\Sigma_s - \omega_s^2\Lambda_{ss} + X_s\frac{\langle f_s(\tilde{\boldsymbol{n}},t)\rangle}{m_s}, \tag{19}$$

$$\frac{dX_s}{dt} = \sum_{j=1}^{3} T_{js}\langle K_j(\tilde{\boldsymbol{x}})\rangle\left[g_{js}(t)X_s - \frac{T_{js}}{\lambda_j}G_j(t)\Lambda_{ss}\right] + Y_s, \tag{20}$$

$$\frac{dV_{ss}}{dt} = \sum_{j=1}^{3} T_{js}\langle K_j(\tilde{\boldsymbol{x}})\rangle\left[g_{js}(t)Y_s - \frac{T_{js}}{\lambda_j}G_j(t)\Sigma_s\right] - \gamma_s Y_s - \omega_s^2 X_s + \frac{\langle F_s(\tilde{\boldsymbol{n}},t)(\tilde{n}_s-\langle\tilde{n}_s\rangle)\rangle}{m_s}, \tag{21}$$

where we define $f_s(\boldsymbol{n},t) = \partial F_s(\boldsymbol{n},t)/\partial n_s$, which is a linear function of $\boldsymbol{n}$, $K_j(\tilde{\boldsymbol{x}}) = e^{-\tilde{\boldsymbol{x}}\cdot\boldsymbol{T}_j/\lambda_j}$ and its mean $\langle K_j(\tilde{\boldsymbol{x}})\rangle = K_j(\langle\tilde{\boldsymbol{x}}\rangle)e^{\boldsymbol{T}_j\boldsymbol{\Lambda}\boldsymbol{T}_j^{\rm T}/\lambda_j^2}$, $\boldsymbol{g}_j(t) = \langle\partial\Gamma_j(\tilde{\boldsymbol{n}},t)/\partial\tilde{\boldsymbol{n}}\rangle$ with $g_{js}(t)$ being the sth component, and $G_j(t) = \langle\Gamma_j(\tilde{\boldsymbol{n}},t)\rangle - \boldsymbol{g}_j(t)\mathrm{diag}(\boldsymbol{T}_j)[X_1,X_2]^{\rm T}/\lambda_j$.

The model can be further refined by the nonlinear resistance and the nonlinear vibration of nanopillars. According to the calculation in Ref. [37], we can add a factor of $(1+\beta_j U_j^2)$ to the conductance $1/R_j^0$ in Eq. (5), where $\beta \propto (d_j/\lambda_j)^2$ if the tunneling length $d_j \gg \lambda_j$.

We can combine the ordinary differential equations Eqs. (11) and (13)–(21) and the mean of Eq. (1) together in order to solve the mean of variables, which can be accomplished numerically. Empirically, the order of moment in Eq. (14) can be set to $l_1 + l_2 \leqslant 4$ for decent accuracy. For nonresonant scenarios, we can simply set $\Lambda_{ss}, W_s, \Sigma_s, X_s$, and Y_s to zero and ignore Eqs. (17)–(21) to reduce the complexity. Another considerable approximation is that a high-quality factor Q for the mean of Eq. (1) may be scaled down to a smaller value by scaling up λ_j, in order to greatly reduce the simulation time, as long as vibration is close to an undamped resonance (the resonant frequency is close to the eigenfrequency, and the electric force is usually balanced by the damping force in the steady state). Details are discussed in Ref. [36].

B. Current

The macroscopic current can be calculated from the mean rate of electrons tunneling:

$$I(t) = C_0\frac{dV}{dt} + q\sum_{j=1}^{3}\kappa_j\langle\Gamma_j(\tilde{\boldsymbol{n}},\tilde{\boldsymbol{x}},t)\rangle, \tag{22}$$

where C_0 is the equivalent capacitance seen from the electrode. In the steady state, $I(t)$ is periodic. Direct current $I_{\rm dc}$ is a time average of $I(t)$ for a full period. As $\langle\tilde{n}_1\rangle,\langle\tilde{n}_2\rangle$, and $V(t)$ are periodic, we can substitute Eq. (11) into Eq. (22) and remove the terms with $\partial\langle\tilde{n}_{1,2}\rangle/\partial t$, thus

$$I_{\rm dc} = \frac{q\omega}{2\pi}\int_{t_0}^{t_0+2\pi/\omega}\langle\Gamma_j(\tilde{\boldsymbol{n}},\tilde{\boldsymbol{x}},t)\rangle\,dt, \tag{23}$$

where $j = 1$, 2, and 3 are equal. The value of $I_{\rm dc}$ is usually small compared to $I(t)$ because the current flows in another direction after half a period π/ω.

An important conclusion about symmetry breaking of the current can be derived from Eq. (9). If $\boldsymbol{n}_{\rm G} = 0$ and $V(t) = -V(t+\pi/\omega)$, we have $\Gamma_j^{\pm}(\boldsymbol{n},\boldsymbol{x},t+\pi/\omega) = \Gamma_j^{\mp}(-\boldsymbol{n},\boldsymbol{x},t)$ from Eqs. (5) and (6), and $F_s(\boldsymbol{n},t+\pi/\omega) = F_s(-\boldsymbol{n},t)$ from Eq. (7). Let us replace t by $t+\pi/\omega$ in Eq. (9) and substitute the above relations into Eq. (9) with $\boldsymbol{n}$ replaced by $-\boldsymbol{n}$. Then we obtain the same equation for $P(-\boldsymbol{n},\boldsymbol{x},\boldsymbol{v},t+\pi/\omega)$ as Eq. (9) indicating $P(\boldsymbol{n},\boldsymbol{x},\boldsymbol{v},t), P(-\boldsymbol{n},\boldsymbol{x},\boldsymbol{v},t+\pi/\omega) = P(\boldsymbol{n},\boldsymbol{x},\boldsymbol{v},t)$ in the steady-state solution. In this case we have $I(t) = -I(t+\pi/\omega)$ from Eq. (22) and no direct current.

Thus, there are two ways to break the symmetry: First is to apply bias on the gate. If $\boldsymbol{n}_{\rm G} \neq 0$, we still have $\Gamma_j^{\pm}(\boldsymbol{n},t+\pi/\omega) = \Gamma_j^{\mp}(2\boldsymbol{n}_{\rm G}\boldsymbol{B}-\boldsymbol{n},t)$, but $F_s(\boldsymbol{n},t+\pi/\omega) \neq F_s(2\boldsymbol{n}_{\rm G}\boldsymbol{B}-\boldsymbol{n},t)$. Thus, $I(t) \neq -I(t+\pi/\omega)$, which enables the direct current. Second is to introduce even-order harmonics in $V(t)$, which breaks the symmetry of AC voltage after half a period, making $V(t) \neq -V(t+\pi/\omega)$. The wave superposition makes use of the nonlinear transport relation. In practice, this could be realized by natural wave distortion, introducing nonlinear elements in the circuit, or magnifying the second-order harmonic by the RF circuit.

In addition, as $e^{-\langle\boldsymbol{x}\rangle\cdot\boldsymbol{T}_j/\lambda_j}$ is periodic with $\omega,\langle\tilde{\boldsymbol{n}}(t)\rangle$ has considerable higher-order harmonic components. Thus, the system resonates when the frequency component is close to both ω_1 and ω_2, so ω should be around ω_1/l where $l = 1,2,3,\ldots$, and smaller l leads to stronger vibrations. This phenomenon is known as Arnold's tongues and was observed in Refs. [31,32].

The direct current, as a key device characteristic, must be obtained from accurate numerical computation, since the

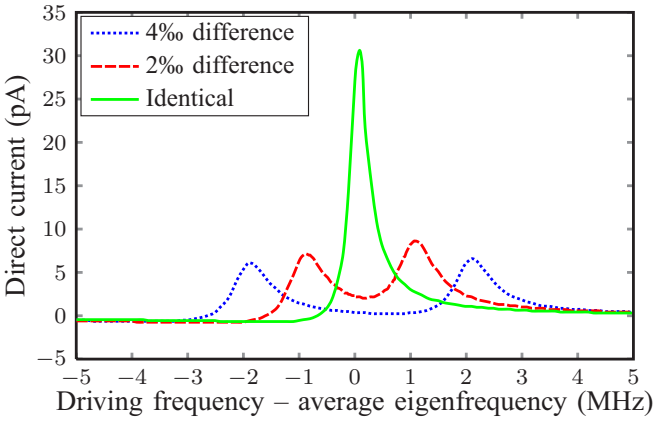

FIG. 2. Direct current versus driving frequency (with an offset of the average eigenfrequency of the two shuttles 500 MHz), when driving amplitude is 1 V and a second-order harmonic with amplitude of 0.5 V introduces asymmetry. The difference of two eigenfrequencies are varied for three curves, indicated in the legend.

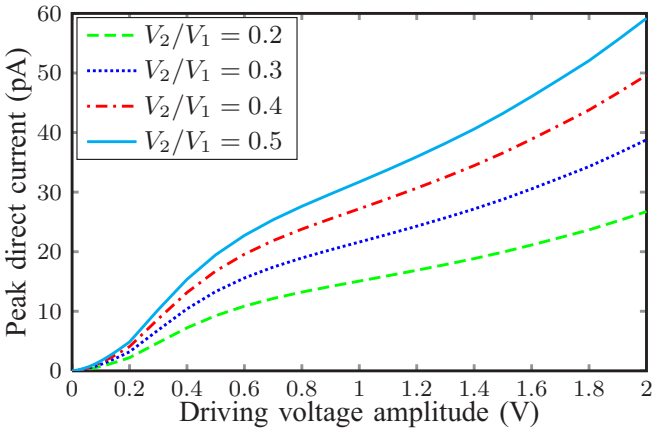

FIG. 3. Peak direct current (over the frequency) versus driving voltage amplitude V_1, with different ratios of second-order amplitude V_2/V_1.

value is usually so small that it is flooded by noise, and therefore it can hardly be acquired from previous methods. Using our fast approximate solution above, Fig. 2 plots a typical resonant response of coupled shuttles, whose geometry follows Ref. [31] (for simulation of capacitance and resistance) and their eigenfrequencies are both around 500 MHz. Here we assume that $V(t) = V_1 \sin(\omega t) + V_2 \cos(2\omega t)$ with $V_1 = 1$ V and $V_2 = 0.5$ V. The second order harmonics (with $\pi/2$ phase difference) introduces asymmetric phases for current of two directions. According to theoretical prediction [37] and to match experimental results in Ref. [31], we assume the tunneling length λ_j is 0.2 Å.

In addition, Fig. 3 shows how the amplitude of driving voltage impacts on the direct current, where V_1 varies from 0 to 2 V and V_2/V_1 varies from 0.2 to 0.5. The quasilinear relation matches the measurement in Ref. [31]. Although the direct current shown here is of the order of 10 pA, 10^9 arrays integrated in a 1 cm^2 area could provide a 10 mA order current, which is useful to drive a device.

IV. CONCLUSION

In conclusion, we have proposed a full stochastic model for the coupled nanomechanical electron shuttles, focusing on the Markovian behavior and the direct output current. By treating the electronic and mechanical motions as stochastic processes, we derive the linear master equation that enables analysis of symmetry breaking. Further results show that even-order harmonics of the driving voltage or a gate bias are necessary for observing a direct signal. Further, we developed the deterministic ordinary differential equations for the mean and covariance of random variables, by assuming the multivariate Gaussian distribution. This provides an efficient method for device-level simulation.

ACKNOWLEDGMENTS

We acknowledge support by the Wisconsin Alumni Research Foundation (WARF) through an Accelerator grant and the Defense Advanced Research Projects Agency (DARPA) through the NEMS-CMOS program (N66001-07-1-2046).

[1] O. Y. Loh and H. D. Espinosa, Nat. Nanotech. **7**, 283 (2012).
[2] L. Y. Gorelik, A. Isacsson, M. V. Voinova, B. Kasemo, R. I. Shekhter, and M. Jonson, Phys. Rev. Lett. **80**, 4526 (1998).
[3] C. Weiss and W. Zwerger, Europhys. Lett. **47**, 97 (1999).
[4] N. Nishiguchi, Phys. Rev. B **65**, 035403 (2001).
[5] A. Isacsson and T. Nord, Europhys. Lett. **66**, 708 (2004).
[6] A. D. Armour, M. P. Blencowe, and Y. Zhang, Phys. Rev. B **69**, 125313 (2004).
[7] A. D. Armour, Phys. Rev. B **70**, 165315 (2004).
[8] F. Pistolesi and R. Fazio, Phys. Rev. Lett. **94**, 036806 (2005).
[9] F. Pistolesi and R. Fazio, New J. Phys. **8**, 113 (2006).
[10] C. Huldt and J. M. Kinaret, New J. Phys. **9**, 51 (2007).
[11] N. Nishiguchi, Phys. Rev. B **78**, 085407 (2008).
[12] L. M. Jonsson, F. Santandrea, L. Y. Gorelik, R. I. Shekhter, and M. Jonson, Phys. Rev. Lett. **100**, 186802 (2008).
[13] J. Wiersig, S. Flach, and K.-H. Ahn, Appl. Phys. Lett. **93**, 222110 (2008).
[14] M. E. Pena-Aza, A. Scorrano, and L. Y. Gorelik, Phys. Rev. B **88**, 035412 (2013).
[15] D. Fedorets, L. Y. Gorelik, R. I. Shekhter, and M. Jonson, Phys. Rev. Lett. **92**, 166801 (2004).
[16] T. Novotny, A. Donarini, and A.-P. Jauho, Phys. Rev. Lett. **90**, 256801 (2003).
[17] T. Novotny, A. Donarini, C. Flindt, and A.-P. Jauho, Phys. Rev. Lett. **92**, 248302 (2004).
[18] Z. Rong, C. Wei-Dong, D. Su-Qing, and Y. Ning, Chin. Phys. B **22**, 117305 (2013).
[19] S. I. Kulinich, L. Y. Gorelik, A. N. Kalinenko, I. V. Krive, R. I. Shekhter, Y. W. Park, and M. Jonson, Phys. Rev. Lett. **112**, 117206 (2014).

[20] M. J. Moeckel, D. R. Southworth, E. M. Weig, and F. Marquardt, New J. Phys. **16**, 043009 (2014).
[21] K. H. Ahn, H. C. Park, J. Wiersig, and H. Jongbae, Phys. Rev. Lett. **97**, 216804 (2006).
[22] M. Prada and G. Platero, Phys. Rev. B **86**, 165424 (2012).
[23] A. Erbe, R. H. Blick, A. Tilke, A. Kriele, and J. P. Kotthaus, Appl. Phys. Lett. **73**, 3751 (1998).
[24] H. Park, J. Park, A. K. L. Lim, E. H. Anderson, A. P. Alivisotos, and P. L. McEuen, Nature (London) **407**, 57 (2000).
[25] A. Erbe, C. Weiss, W. Zwerger, and R. H. Blick, Phys. Rev. Lett. **87**, 096106 (2001).
[26] D. V. Scheibe and R. H. Blick, Appl. Phys. Lett. **84**, 4632 (2004).
[27] D. R. Koenig, E. M. Weig, and J. P. Kotthaus, Nat. Nanotech. **3**, 482 (2008).
[28] D. V. Scheible and R. H. Blick, New J. Phys. **12**, 023019 (2010).
[29] D. R. Koenig and E. M. Weig, Appl. Phys. Lett. **101**, 213111 (2012).
[30] H. S. Kim, H. Qin, and R. H. Blick, New J. Phys. **12**, 033008 (2010).
[31] C. Kim, J. Park, and R. H. Blick, Phys. Rev. Lett. **105**, 067204 (2010).
[32] C. Kim, M. Prada, and R. H. Blick, ACS Nano **6**, 651 (2012).
[33] C. Kim, M. Prada, G. Platero, and R. H. Blick, Phys. Rev. Lett. **111**, 197202 (2013).
[34] C. Kim, M. Prada, H. Qin, H.-S. Kim, and R. H. Blick, Appl. Phys. Lett. **106**, 061909 (2015).
[35] R. I. Shekhter, L. Y. Gorelik, M. Jonson, Y. M. Galperin, and V. M. Vinokur, J. Comput. Theor. Nanos. **4**, 860 (2007).
[36] M. Zhao and R. H. Blick, arXiv:1405.1645.
[37] J. G. Simmons, J. Appl. Phys. **34**, 238 (1963).